Wealth of Knowledge Frozen in Time: Innovative Breakout Shell Autopsy

Jackie Leung[1] and Joydeep Sengupta[1]

[1]ArcelorMittal - Global R&D Hamilton
1390 Burlington Street East, Hamilton, ON. L8N 3J5 Canada
Phone: 905-548-4759
E-mail: jackie.leung@arcelormittal.com

Key words: Continuous Casting, Breakouts, Laser Scanning Profilometry, Hangers, Sticker Breakouts, Oscillation Marks

INTRODUCTION

ArcelorMittal Dofasco (AMD) has two steel producing streams (Figure 1). The KOBM stream uses one basic oxygen furnace where the tapped heats are refined at the ladle-metallurgy facility (LMF 1) and cast at the No. 1 continuous caster (1CC); some grades are processed at the tank degasser prior to casting. The electric arc furnace (EAF) stream uses a twin shell EAF, where the tapped heats are refined at LMF 2 and cast at 2CC. Several different grades are produced between the two streams, which include: ultra low carbon, low carbon, medium carbon, high carbon, HSLA, and dual phase steels.

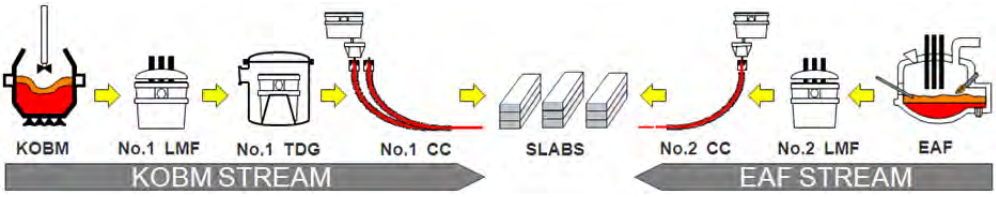

Figure 1. ArcelorMittal Dofasco steelmaking process diagram

In order to maximize caster productivity, unscheduled delays must be reduced. A breakout is a detrimental unscheduled delay at the caster which causes damage to equipment and reduces productivity. Root cause of the breakout must be correctly determined to implement corrective action and prevent reoccurrence. However, breakouts are complicated, often caused by localized interactions between fluid flow, heat transfer, solidification phenomena, and mechanical effects due to equipment. If the artifacts of these effects are absent in the process signals, or hidden by debris at the breakout location on the slab, determination of root cause is not straightforward. Furthermore, different circumstances lead to dissimilar types of breakouts that require different methods and techniques to gather evidence to correctly determine root cause.

The concept of caster breakout and methods of breakout prevention has been well-documented.[1] However, published case studies of actual caster breakouts and characterization techniques are few and far in between. Blazek and Saucedo[2] inspected the as-cast surface of a sticker-type breakout shell. Similarly, Misra *et al.*[3] inspected the as-cast surface of a hydrogen-induced sticker-type breakout shell and mould slag found between the shell and mould wall. Singh *et al.*[4] inspected the interior and exterior as-cast surfaces of several breakout shells. They also cut the shells into sections to visually inspect the transverse cross-sections and qualitatively evaluate shell thickness. Santillana *et al.*[5] applied 3D laser scanning profilometry on two breakout shells to measure shell thickness for quantitative analysis. Stransky *et al.*[6] examined macro-structure by deep etching, and quantified chemical heterogeneity by undisclosed chemical composition testing near the breakout location. Iwasaki and Thomas[7] measured area of the breakout hole to calculate the time to drain the liquid steel from the shell. They also deep etched a slab sample cast 5 m preceding the breakout event to demonstrate shell thinning in the breakout position.

In this paper, various techniques routinely used at Global R&D Hamilton to support breakout investigations are demonstrated by three case studies. The specific root causes are not the focus of this paper, but rather the innovative techniques that were used to analyze the shells. Techniques were mostly applied to the breakout shells since casting conditions which led to the breakout can be “frozen” at the shell. Clues from the breakout shell must be discovered and interpreted much like an autopsy. Similar to an autopsy, findings provide direction for the investigation to be carried out at other parts of the slab or caster.

CASE 1: BREAKOUT ON A HSLA GRADE

This case study describes the benefit of sandblasting the breakout shell to reveal intricate details of oscillation marks and surface features. Additionally, an ultrasonic flaw detecting device was used to quickly measure shell thickness which was compared to CON1D[8] prediction. Lastly, metallographic analysis was used to identify unknown material found in the slab.

Surface Inspection after Cutting and Sandblasting

The breakout shell had fractured into two pieces during the breakout. Piece #1 (mould shell) remained inside the mould and Piece #2 (slab shell) was attached to the slab (refer to schematic in Figure 2). Global R&D Hamilton had retained the mould shell for analysis. The mould shell was cut into smaller pieces using a hand-torch cutter and laid out flat (Figure 2). As seen in the figure, the fracture edges on both broad faces are angled ~36° and converge onto the northeast edge. This angled fracture edge indicates a sticker-type breakout,[3] originating from the top (inner radius) broad face near the northeast edge.

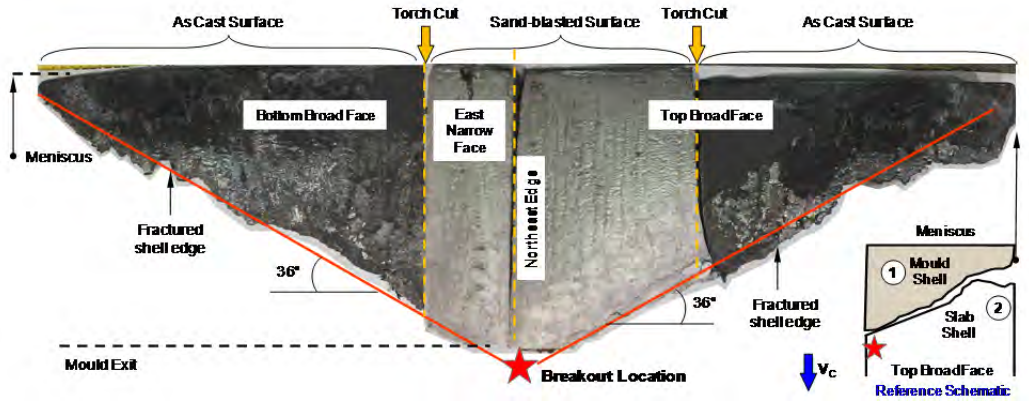

Figure 2. Mould shell after torch cutting and laid out flat

An additional benefit of cutting the mould shell to smaller pieces was so the pieces could be placed into a sandblasting chamber. Sandblasting removes the scale and greatly improves the visibility of the surface features of the shell, but this process is quite labor-intensive. Therefore, only pieces of interest were selected to be sandblasted. The contrast in appearance between the as-cast surface with scale, and the sandblasted surface with scale removed is shown in Figure 2.

Sandblasting the broad face surface revealed intricate details (Figure 3). Breakout shell observations that were made clear:

1. The meniscus edge was very thick and irregular;
2. There were multiple longitudinal depressions along the broad face;
3. Oscillation marks were flattened out at the vicinity of the fracture edge;
4. Oscillation marks near the fracture edge were closely spaced and curved toward the breakout location.

These irregular and abnormal features on the shell indicated a sticker formation and propagation inside the mould.[9]

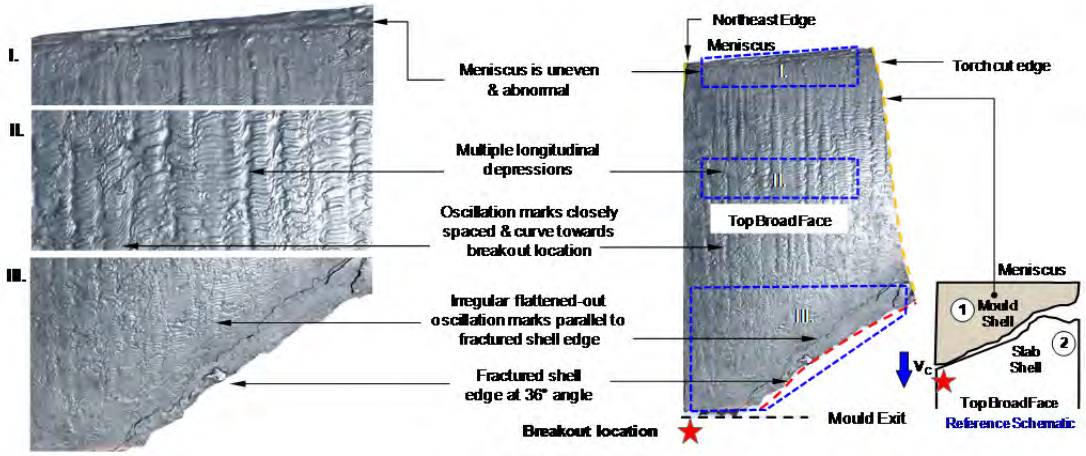

Figure 3. Breakout shell from mould after sandblasting

Shell Thickness Measurement and Model Comparison

Measurement of the shell thickness was needed to quantify the abnormal meniscus and thinning near the fracture edge. Typically, a cross-section of the shell would be cut out and thickness would be measured using a ruler or calipers. However, cutting out the shell slab in the slab yard would have been time and labor-intensive. Therefore, an improved technique was applied to measure shell thickness quickly and effectively. A portable ultrasonic flaw detecting device, typically used for non-destructive testing of defects in products, was used to measure thickness of the breakout shell along the casting direction (Figure 4). A relatively flat surface was required for measurement, but when calibrated with standards of known thickness, the ultrasonic flaw detecting device provided quick and accurate thickness measurements. The device is more complex than a ruler or calipers. Hence, the signal needs to be properly interpreted by a trained operator. The device was both portable and durable so that it could be brought to the slab yard for *in-situ* measurements so additional cutting of the shell was not required. Similar ultrasonic measurements were made on the mould shell for consistency of measurement technique.

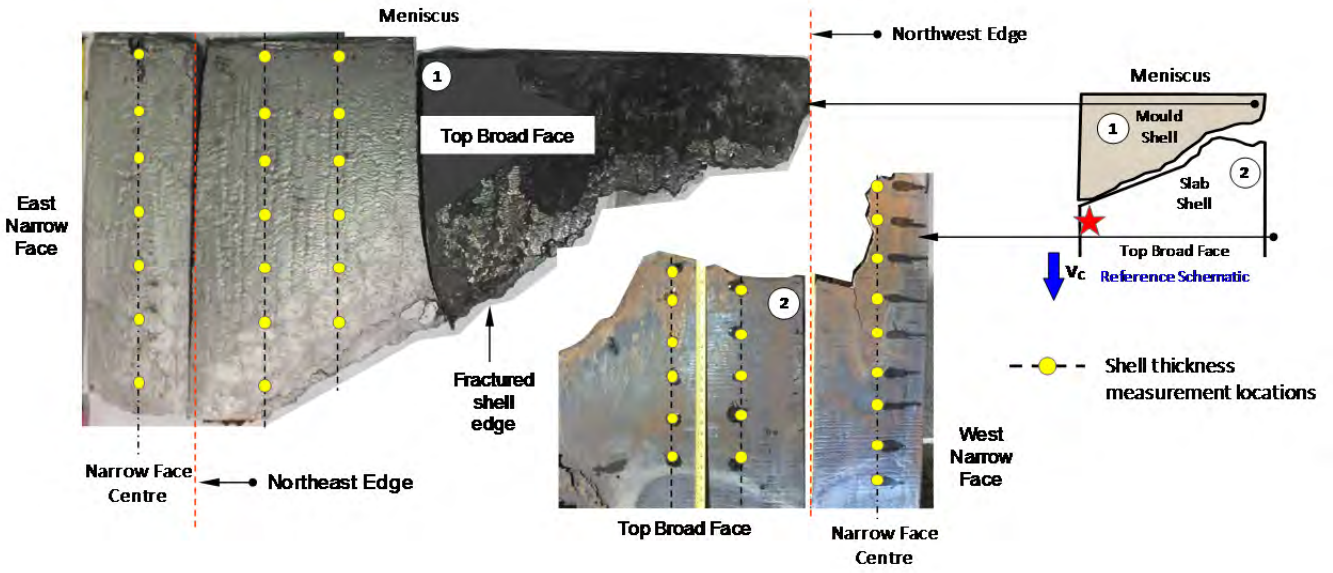

Figure 4. Ultrasonic measurement locations on shell from mould and slab

The shell thickness profiles were compared with CON1D prediction (Figure 5). From Figure 5a, the mould shell was thicker at the meniscus and thinner at the fracture edge near mould exit compared with CON1D. The shell was the thinnest near the fracture edge of the east narrow face centre, indicating the breakout originated from near this location. From Figure 5b, the thickness profile on the west narrow face centre, farthest away from the breakout location, has good agreement to CON1D. Therefore, shell growth at this location followed normal solidification behavior. However, the shell becomes thinner along the fracture edge. This is typical shell thickness behavior seen on breakout shells after a sticker breakout.

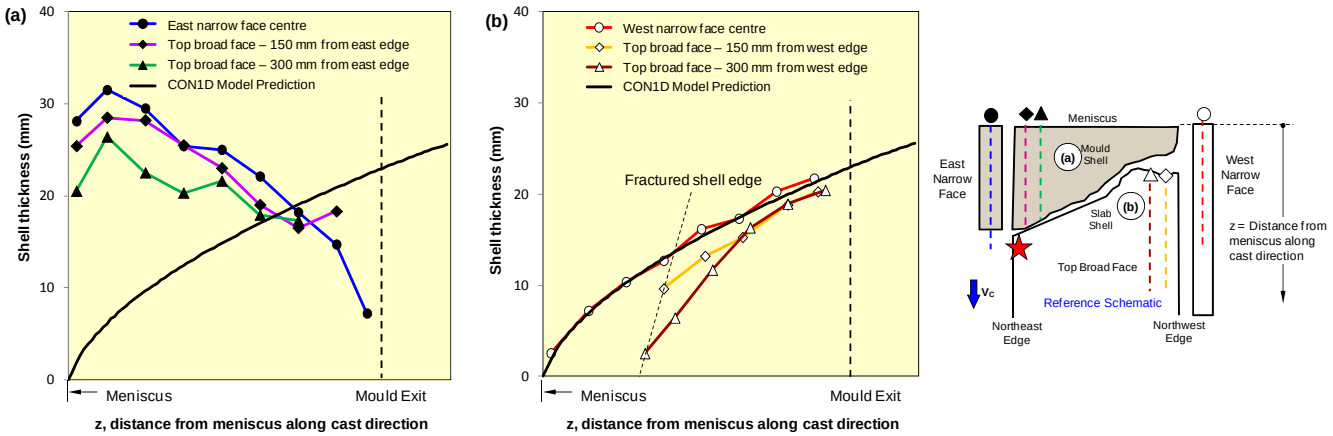

Figure 5. Thickness profiles for (a) mould shell and, (b) slab shell with CON1D model prediction

Additional Observations and Metallography

Sandblasting also revealed an abnormal feature below the meniscus on the mould shell (Figure 6a). A distinctive imprint along the northeast edge indicates a foreign object pushed up against the shell during the breakout. A similar imprint was observed on the slab on the same edge ~9 m below the meniscus (Figure 6b). The object was referred to as a "hanger" because it sticks and hangs onto the mould, but differs from a sticker because it is not part of the shell.

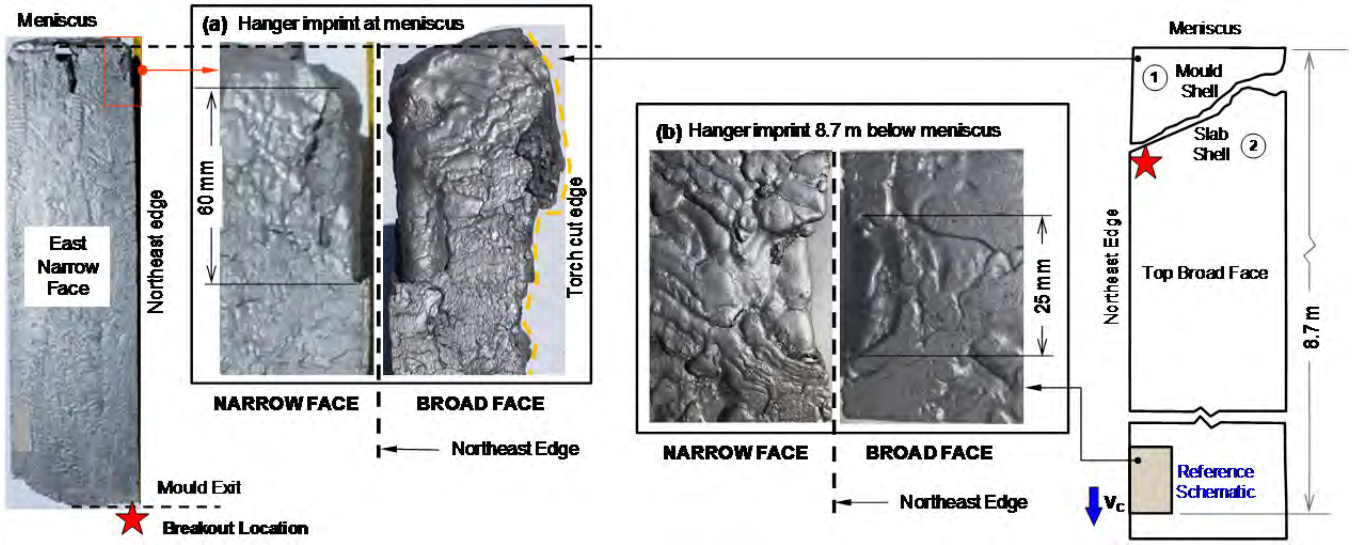

Figure 6. (a) Hanger imprint at meniscus, (b) Hanger imprint on breakout slab

Another atypical feature was observed near the hanger imprint ~9 m below the meniscus. A section of this feature was cut and the transverse cross-section surface was milled for further analysis (Figure 7a). The cross-section revealed a secondary shell on the northeast corner of the slab. This was a piece of the hanger that detached with that portion of the slab. Scanning Electron Microscope Energy-Dispersive X-ray Spectroscopy (SEM-EDS) was applied and detected elements consistent with mould powder (Figure 7b). An entrapped particle was observed 5.5 mm beneath the top broad face surface (Figure 7c). SEM-EDS of the particle also detected elements consistent with mould powder. CON1D was used to determine that at 5.5 mm below the broad face surface, the particle was embedded on the shell 80 mm below the meniscus during casting.

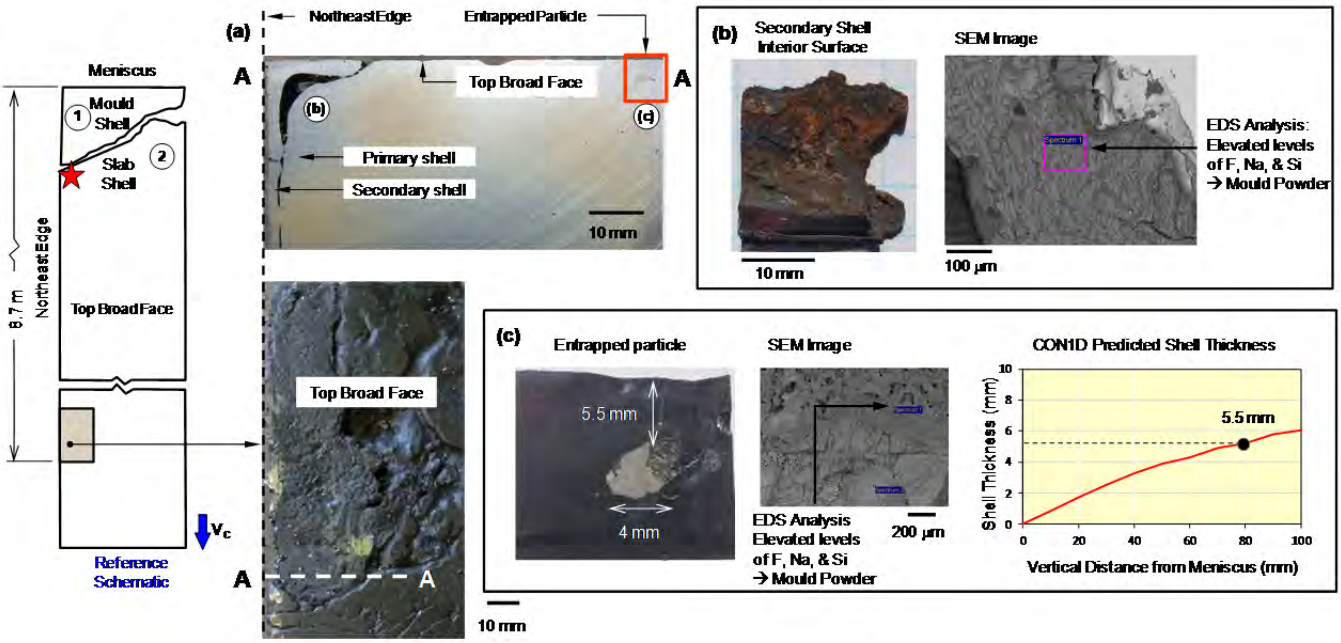

Figure 7. (a) Abnormal feature on breakout slab; Analyses of (b) hanger interior surface and, (c) entrapped particle

CASE 2: BREAKOUT ON A LOW-CARBON GRADE

This case study describes the innovative use of a portable 3D laser scanning profilometer on a breakout shell and the capability of the device's post-processing software which provided a wealth of knowledge about the breakout. The laser scanner is mounted on a portable 7-axis articulating arm which measures the co-ordinates of the scanned object's surface. Shell surface profilometry can be acquired quickly, accurately, and with higher resolution than the methods described in the previous case. Additionally, extraction and visualization of data by the post-processing software is also described.

The breakout shell was hand-torch cut from the slab and into smaller pieces. Pieces of interest were sandblasted and scanned using the laser profilometer to acquire a digital copy of the shell (Figure 8a). The software could digitally acquire multiple cross-sections of the scanned breakout shell without having to spend the time or labor to manually cut and measure the shell (Figure 8b). From this figure, it can be seen that Section D experienced localized shell thinning near the breakout position and that corner shape of the southwest corner near the breakout position was clearly different from the southeast corner.

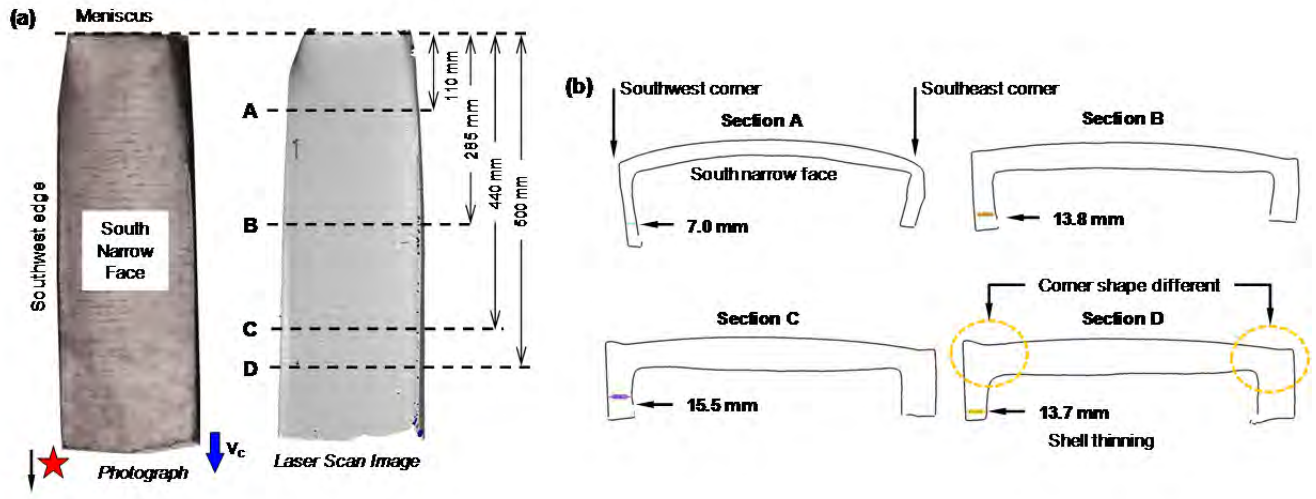

Figure 8. (a) Comparison of photograph and 3D laser scan of breakout shell; (b) digital transverse shell cross-sections

The software was used to acquire co-ordinates for selected cross-sections of the breakout shell. Thickness profiles of the narrow and broad face centrelines were compared to the profile at the breakout position (Figure 9a). From this figure, the shell thickness at the surface depressions are up to 50% thinner than the same position at the narrow and broad face centrelines. The software was used to quickly calculate thickness profile of the scanned piece and visualize the data as a color contour map (Figure 9b). From this figure, it can be seen that there were thin spots in line with the breakout position which corresponded to the locations of observed surface depressions.

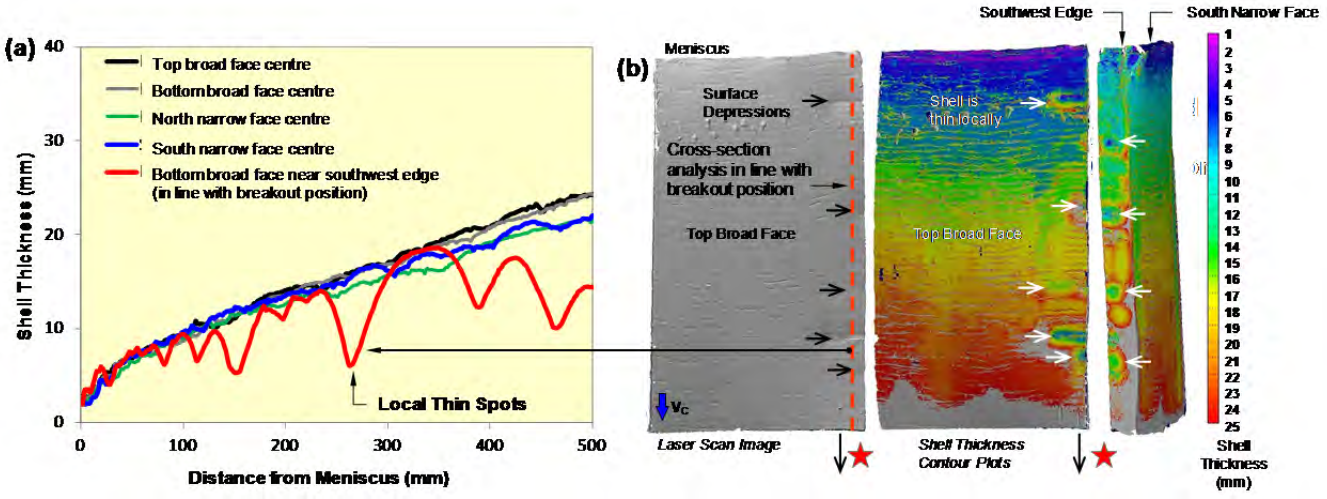

Figure 9. (a) Thickness profiles of breakout shell, (b) Laser scan of breakout shell with thickness color contour plots

CASE 3: BREAKOUT ON A MEDIUM-CARBON GRADE

This case study describes an innovative method to inspect the interior shell surface using a camera and an inspection pole. Metallography and fractography were used to analyze a crack observed on the shell. Findings from the shell directed the investigation to the segment rolls where unknown material was observed. SEM-EDS analysis was used to determine the nature of that material. Data from thermomechanical testing of this grade was also used in the investigation.

Interior Shell Inspection

A breakout shell ~3 m in length was retained at the caster to determine if samples were required. Surface inspection revealed several depressions and longitudinal cracks in line with the breakout position (Figure 10a). To determine if the longitudinal crack was responsible for creating the breakout hole, it was necessary to inspect the interior shell surface, which was conventionally unreachable. It would have been very time and labor-intensive to cut the entire breakout shell into manageable pieces. Therefore, a digital camera attached to a pole was used to inspect the interior shell surface along the crack position. The longitudinal crack was visible in several locations along the interior of the breakout shell (Figure 10b). From the figure, the middle image shows the rounded crack edge which indicates that the crack had occurred during the breakout and not after. Areas of interest were selected to be cut out for further analysis.

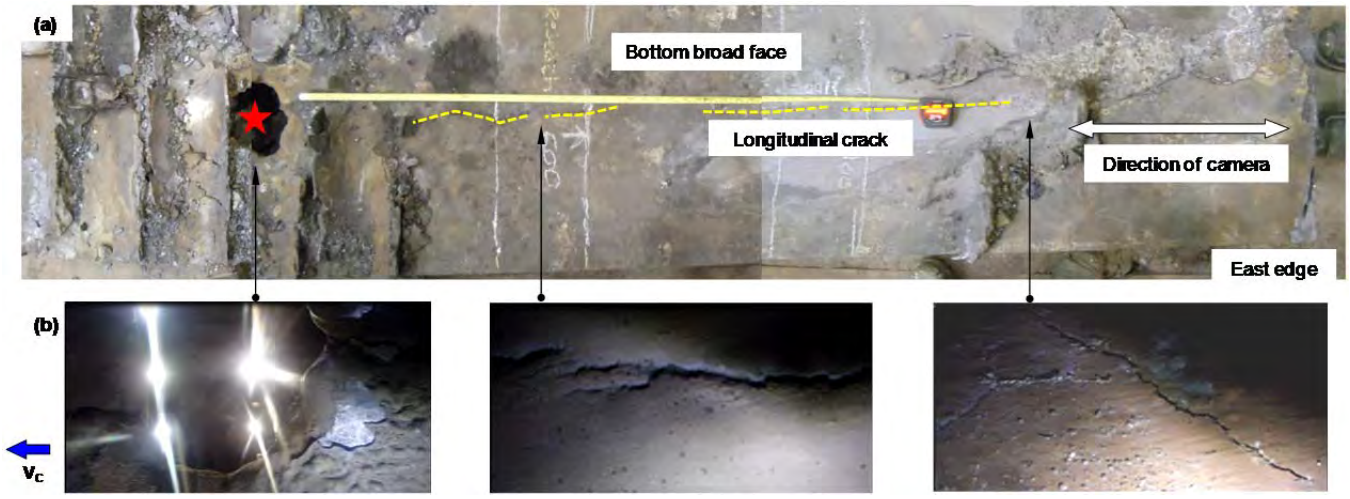

Figure 10. (a) Breakout shell, (b) Images from camera inspection of interior surface of shell

Fractography

A section with a longitudinal crack was removed from the shell (Figure 11a). The fracture surface was sandblasted and examined (Figure 11b). The fracture surface shows two distinctive patterns of fracture: low and high temperature. The low temperature fracture is typical of a brittle fracture. In the high-temperature fracture, the imprint of primary dendrites formed during casting is clearly visible. This indicates that the crack occurred at high temperature during casting.

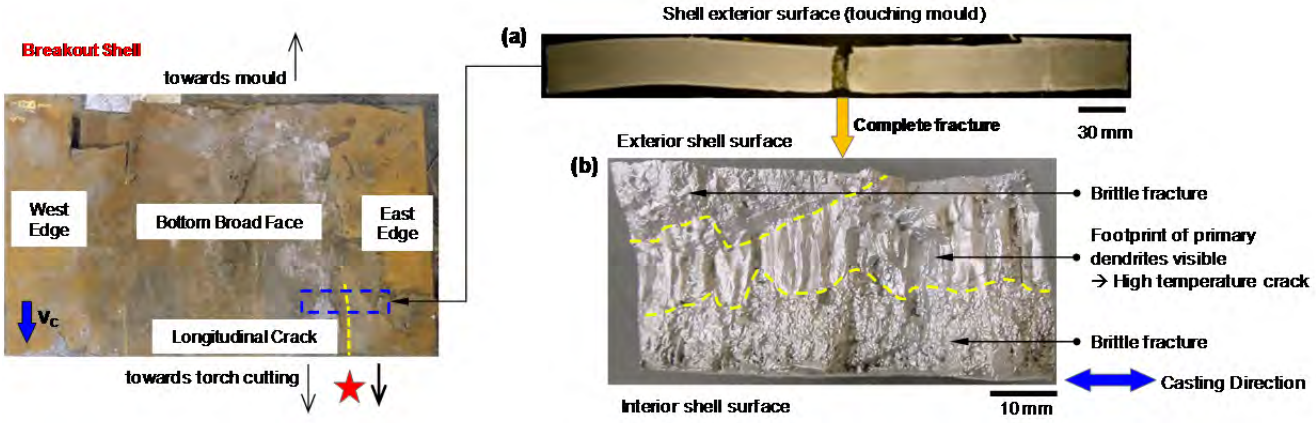

Figure 11. (a) Sample from breakout shell with crack, (b) Fracture surface after sandblasting

Crack Formation and Thermomechanical Testing

The sample from Figure 11(a) was deep etched[10] to reveal the macrostructure. Several shallow internal cracks were observed beneath a surface depression (Figure 12a). The shell cross-section is divided into three zones: Area 1 - from exterior shell surface to crack start, Area 2 - from crack start to crack end, and Area 3 - from the crack end to interior shell surface. Using CON1D, these cracks were initiated ~1.5 m below the meniscus. CON1D also predicted the thermal profile of the shell at that machine location (Figure 12b). It indicates that the temperature of the area when the crack formed was at ~1400°C. Thermomechanical testing of this particular grade showed reduced fracture stress at such as high temperature (Figure 12c), making the area more susceptible to cracking.

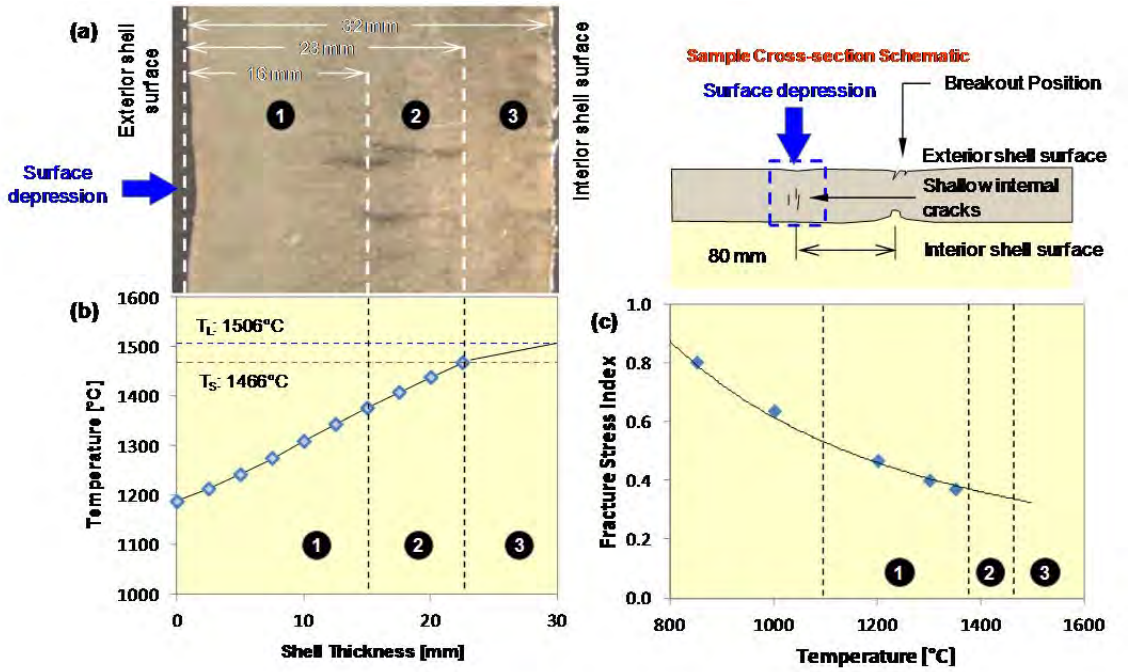

Figure 12. (a) Macrostructure of breakout shell 80 mm from breakout position, b) Shell thermal profile according to CON1D prediction, c) Temperature & Fracture stress relationship for grade

Metallography of Buildup Material

The clues from the shell directed the investigation to the segment rolls near the breakout location. A significant amount of material was found built up on several rolls on the same side as the breakout hole (Figure 13a). SEM-EDS showed that the buildup material formed in layers (Figure 13b), and the different layers revealed elements consistent of scale and mould powder slag (Figure 13c).

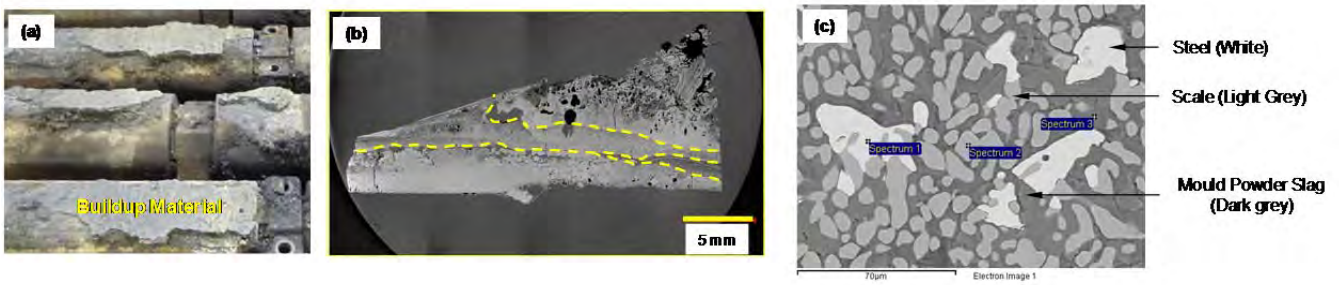

Figure 13. (a) Buildup material on segment rolls, (b) cross-section of buildup material, (c) SEM analysis of buildup material

SUMMARY & CONCLUSIONS

Three case studies of breakouts each with unique root causes were discussed. A variety of innovative techniques were used to analyze the breakout shells and collect quantitative data. Findings from the detailed analyses were used to determine the root causes. Several conclusions are made:

1. Breakout shells contain features and characteristics that reflect casting conditions during the breakout event.
2. Findings from the breakout shell give direction to the investigation when resources are limited.
3. Shell thickness measurement via ultrasonic or 3D laser scanning profilometry provides quantitative data.
4. Metallographic and chemical analysis techniques identify unknown materials.
5. Thermal models provide key information related to abnormal shell behavior.
6. Deep etching reveals macrostructure and shows features related to shell formation.
7. Thermomechanical testing combined with thermal models is an innovative method to understand crack formation.

ACKNOWLEDGEMENTS

The authors would like to thank their colleagues at ArcelorMittal Dofasco and Global R&D Hamilton for their support: S. Chung, T. Rayner, N. Strobl, N. Mayo, B. Sulatycky, M. Trinh, L. Stewart, J. Daw, L. Sun, A. Marino, S. Tupper, A. Chang, M. McHugh, M. Lubrick, P. Kilgannon, A. Weddum (retired), and D. Lilliman (retired).

DISCLAIMER

Please note that the information provided in this article is provided without warranty of any kind, express or implied, and is not a recommendation of any product, process, technique or material nor is it a suggestion that any product, process, technique, or material should not be used. Neither ArcelorMittal Dofasco nor any of its affiliates or employees will be liable for any damage suffered as a result of use of any information provided in this article. Use of any information in this article is entirely at the user's risk. The publication of this paper does not grant any license or other right in respect of any intellectual property owned by ArcelorMittal Dofasco or any of its related companies.

REFERENCES

1. W.H. Emling, "Breakout Prevention," *The Making, Shaping, and Treating of Steel: Casting Volume*, AIST, Warrendale, PA., 2010, pp. 775-808.
2. K.E. Blazek and I.G. Saucedo, "Characterization of the Formation, Propagation, and Recovery of Sticker/Hanger Type Breakouts," *ISIJ International*, vol. 30 (1990), No. 6, pp.435-443.
3. S. Misra, Y. Li, and I. Sohn, "Hydrogen and Nitrogen Control in Steelmaking at U.S. Steel," *Iron and Steel Technology*, November 2009, vol. 6, no. 11, pp. 43-52.
4. R.J. Singh, D. Lal, S.K. Jha, S.Shekhar, E.Z. Chacko, and R. Sahu, "Effect of Different Parameters on Breakouts in Billet Caster," *TMS 2014*, San Diego, California, February 16-20, 2014, pp. 219-229.
5. B. Santillana, B.G. Thomas, G. Botman, and E. Dekker, "3D Thickness Measurement Technique for Continuous Casting Breakout Shells," *7th European Continuous-Casting Conference, 2011*, MetTec InSteelCon, (Dusseldorf, Germany, June 27-July 1, 2011), 2011.
6. K. Stransky, J. Dobrovska, F. Kavicka, M. Masarik, B. Sekanina, and J. Stetina, "Heterogeneity of Continuously Cast Steel Slab Shortly Before Breakout," *METAL 2012 Conference Proceedings*, Brno, Czech Republic, May 2012, Ostrava, Tanger, 2012, pp. 148-153.
7. J. Iwasaki and B.G. Thomas, "Thermal-Mechanical Model Calibration with Breakout Shell Measurements in Continuous Steel Slab Casting," *TMS 2012 - Supplemental Proceedings*, 2012.
8. J. Sengupta, M. Trinh, D. Currey, and B.G. Thomas, "Utilization of CON1D at ArcelorMittal Dofasco's No. 2 Continuous Caster for Crater End Determination," *AISTech 2009 – Iron and Steel Technology Conference Proceedings*, Vol. I, Association of Iron and Steel Technology, USA, 2009, pp. 1177-1185.
9. E.S. Szekeres, Brimacombe Continuous Casting Course, vol. 1, Section J, 2013, pp. 22-24.
10. J. Sengupta, J. Casey, B. Nelson, D. Crosbie, G. Kladnik, and N. Gao, "Qualitative and Quantitative Techniques for Evaluating Manganese Segregation in Advanced High Strength Steels at ArcelorMittal Dofasco's No. 1 Continuous Caster," AISTech 2011 Steelmaking Conference Proceedings, (Indianapolis, IN, May 2-6, 2011), AIST, Warrendale, PA, Vol. 2, 2011, pp. 731-740.